

Spectroscopic Studies of Two Dynamically Different 1,4-Dihydropyridine Structures*

by E. Śliwińska¹, K. Palewska¹, A. Lewanowicz¹, J. Lipiński¹,
J. Sworakowski¹, R. Gancarz² and S. Nešpůrek³

¹*Institute of Physical and Theoretical Chemistry, Wrocław University of Technology,
Wybrzeże S. Wyspiańskiego 27, 50370 Wrocław, Poland*

²*Institute of Organic Chemistry, Biochemistry and Biotechnology, Wrocław University of Technology,
Wybrzeże S. Wyspiańskiego 27, 50370 Wrocław, Poland*

³*Institute of Macromolecular Chemistry, Academy of Sciences of the Czech Republic,
162 06 Prague, Czech Republic*

(Received June 22nd, 2001)

Results of spectroscopic studies of solutions of two photoactive dihydropyridine derivatives: 1-methyl-2,4,4,6-tetraphenyl-1,4-dihydropyridine and 4,4-(biphenyl-2,2'-diyl)-2,6-diphenyl-1-methyl-1,4-dihydropyridine (hereafter referred to as DHP and BDH, respectively) are presented. The analysis of UV-Vis and NMR spectra points to a different behaviour of the two molecules under study, in spite of a close similarity of formal molecular structures. These results indicate that two isomers of BDH exist in solid matrices, as well as in liquid solutions, in the temperature range studied. No such feature has been detected in DHP. We attribute the difference to an enhanced stiffness of the BDH molecule resulting from a bridge between side phenyl groups.

Key words: dihydropyridine, UV-Vis spectroscopy, NMR spectroscopy

Substituted dihydropyridines belong to a family of molecules (*cf.* Fig. 1a) whose representatives have been reported to exhibit photochromic properties in the solid state as well as in solutions (see, *e.g.*, [1–3] for reviews and references). Molecular mechanisms for colouring and bleaching reactions have been postulated: in the former process the initial step was assumed to involve an intramolecular phenyl shift [4–6] and/or a 3,5-bridge formation [7–10]. It has also been believed that initial stages of the photochromic process are identical, irrespective of the nature of the heteroatom in the central ring.

Our earlier research [11–14] was carried out on 1-methyl-2,4,4,6-tetraphenyl-1,4-dihydropyridine (hereafter referred to as DHP – *cf.* Fig. 1b), and on its phenyl-bridged analogue, 4,4-(biphenyl-2,2'-diyl)-2,6-diphenyl-1-methyl-1,4-dihydropyridine (BDH – Fig. 1c). Basing on spectroscopic measurements, isothermal and non-isothermal kinetic experiments, as well as on quantum-chemical calculations, we put forward a scheme explaining the photochemical activity of substituted dihydropyridines. Our results indicate that the initial step of the sequence of elemen-

* Dedicated to the memory of Professor Krzysztof Pigoń.

tary processes following the excitation of the stable form of DHP, rather than a purely intramolecular process assumed earlier [4–10], may be a scission of the bond between one of the phenyls in position 4 and the central ring, followed by formation of radicals. In the context of the mechanism of the photochemical reactions postulated for DHP, it was interesting to compare its properties with those of BDH in which, for structural reasons, a complete separation of the phenyl moiety from the central ring is impossible. Earlier work [11–14] showed that features of the photochemical activity (*e.g.*, activation energies and enthalpies of bleaching reactions, barriers for intramolecular reactions determined from quantum chemical calculations) are similar for both materials. Molecular mechanisms of the colouring and bleaching reactions must, however, differ in details: for structural reasons, formation of the pair of radicals and their subsequent recombination, postulated for DHP [12], is impossible in BDH [13], due to the chemical bond linking two phenyls attached to the central ring in position 4 (*cf.* Fig. 1).

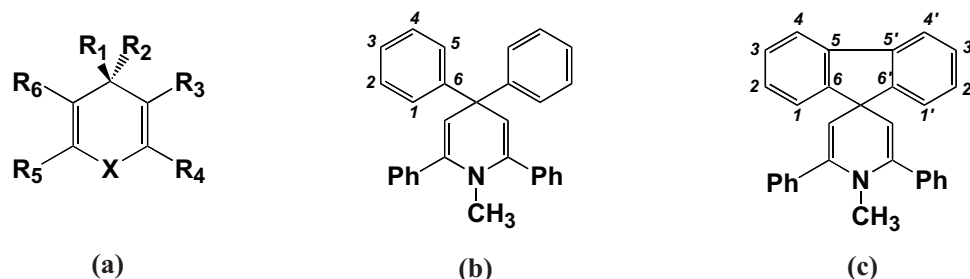


Figure 1. Chemical formulae of stable forms of photochromic compounds. (a) The family of compounds under study ($X = O, S, NR_7$; $R_1, R_4, R_5 = \text{aryl}$; $R_2 = CH_3, \text{aryl}$; $R_3 = H, CH_3$; $R_6 = H$; $R_7 = H, \text{alkyl}$); (b) 1-methyl-2,4,4,6-tetraphenyl-1,4-dihydropyridine (DHP); (c) 4,4-(biphenyl-2,2'-diyl)-2,6-diphenyl-1-methyl-1,4-dihydropyridine (BDH). The numbers in (b) and (c) label protons of the side groups.

X-ray experiments performed on DHP [15] and on other members of the group (see [2] for references) demonstrated that the molecules are non-planar, the central ring assuming a boat conformation. A similar conformation is likely to be assumed by isolated molecules, as has been confirmed by quantum-chemical calculations [8, 11, 12]. These results, however, tell little about the behaviour of lateral groups, their orientations and dynamics. The answer can be sought in spectroscopic studies: in contrast to numerous papers reporting on the photochemical activity of the molecules under study, much less attention has been paid to their spectroscopic properties [9]. Taking into account the non-planarity of the molecules [15], their flexibility and susceptibility to external factors, it seemed interesting to carry out a more thorough study.

EXPERIMENTAL

Absorption spectra were measured with Shimadzu 2101PC and Shimadzu 2401PC UV-Vis spectrophotometers, the latter one supplied with a liquid N_2 cryostat. Glass-forming 3-methylpentane was used as solvent, the concentrations of solutions, carefully de-oxygenated prior to measurements, being of the

order of 10^{-5} M. Luminescence measurements were carried out on a fluorescence spectrophotometer Hitachi F-4500. The two-dimensional spectra were measured by sequentially recording the emission spectra at various excitation frequencies. The spectral resolution was the same in excitation and emission and amounted to 2 nm. Concentrations of the solutions ranged between 10^{-5} and 10^{-4} M. The solutions, in quartz tubes, were placed in an Oxford Instruments DN1704 cryostat, previously cooled down to *ca.* 100 K. The temperature of the samples decreased rapidly to about 120 K, then they were slowly cooled down to 77 K. Apart from the emission and excitation spectra, the F-4500 spectrofluorimeter allowed to measure phosphorescence lifetimes. Fluorescence lifetimes were measured with a LIF200 pulse fluorometer [16]; with samples were excited with a 337 nm line of a nitrogen laser with pulse half-width of *ca.* 1 ns. NMR spectra were recorded using a Bruker Avance DRX 300 FT NMR and a Bruker Avance DRX 500 FT NMR spectrometers equipped with a variable temperature probe, using perdeuterated chloroform, benzene or toluene as solvents.

The details of synthesis and purification of BDH and DHP have been given in [7,8,17]. All organic solvents used in UV-Vis spectroscopy (Merck, UV spectroscopic grade) and in NMR (perdeuterated solvents, Aldrich, 99+%) were used without further purification.

RESULTS AND DISCUSSION

Quantum-chemical calculations: The calculations were carried out in order to determine the energies of the ground and low-lying excited states of DHP and BDH. In most cases, the calculations were performed for optimized geometries of the molecules, in some cases, however, the effect of deformation of the central moiety was also examined.

The ground-state geometries of DHP and BDH were fully optimized using the semiempirical MNDO method of Dewar and Thiel [21], whereas energies of excited states were calculated using the semiempirical GRINDOL method [23], particularly suitable in this type of calculations. 200 singly excited configurations were included into the configuration interaction scheme. The energies of the low-lying electronic transitions of the molecules under study are given in Table 1. Our results are in a reasonable agreement with the earlier ones [8].

Absorption spectra: The absorption spectra of 3-methylpentane solutions of DHP are shown in Fig. 2. In the spectral range covered, the spectra consist of three broad structureless bands, with their onsets at *ca.* 30000 cm^{-1} , 37000 cm^{-1} and 45000 cm^{-1} , and maxima at *ca.* 34800 cm^{-1} , 42200 cm^{-1} and 50000 cm^{-1} . It is interesting to note that principal features of the spectra do not substantially change upon cooling the samples to nitrogen temperatures.

The absorption spectra of BDH are shown in Fig. 3. In contrast to the spectra of DHP, they contain a few discernible peaks commencing above 32000 cm^{-1} , superimposed on a set of broad bands (*cf.* Table 1). Also in this case, apart from an enhanced scattering, there is no qualitative change of the spectra on lowering the temperature.

Luminescence: Luminescence spectra of DHP were measured in Shpol'skii matrices, the best resolution being achieved using n-heptane as solvent; a spectrum in n-heptane is shown in Fig. 2. The fluorescence spectrum begins with a strong line at $\nu_{\text{em}} = 29380\text{ cm}^{-1}$ which can be attributed to the 0-0 of the $S_1 \longrightarrow S_0$ transition (see *infra*). A few vibrational modes associated with this transition can also be distinguished. The second group of emission lines is red-shifted by about 5700 cm^{-1} ; we

Table 1. Calculated and experimentally determined energies of electronic transitions in DHP and BDH. The numbers printed in italics are frequencies tentatively attributed to vibronic transitions within the lowest singlet manifolds. All frequencies are in cm^{-1} .

DHP			BDH				
Calculated frequencies	f	Experimental frequencies (Excitation spectrum)	Structure 'A'		Structure 'B'		
			Calculated frequencies	f	Calculated frequencies	f	
S1	33564	29410 <i>30080</i> 30530 <i>30810</i> <i>31410</i>	S1, 'A'	0.0095	32799	0.0298	29590 <i>30040</i>
S2	33887	32160 <i>32790</i>	S1, 'B'	0.0009	34117	0.0125	30940 <i>32740</i> 32740
S3	37918	35200	S2	0.0001	35199	0.2723	34250
S4	37983	37500	S3	0.0006	35979	0.0003	35450
S5	38016	38820	S4	0.0003	37951	0.0011	36350
S6	39476	40500	S5	0.5098	37988	0.0007	37260
S7	40994		S6	0.0541	39679	0.6088	39360
T1	24296		S7		40871	0.0113	40190
		
			S14		47112	1.0324	46730

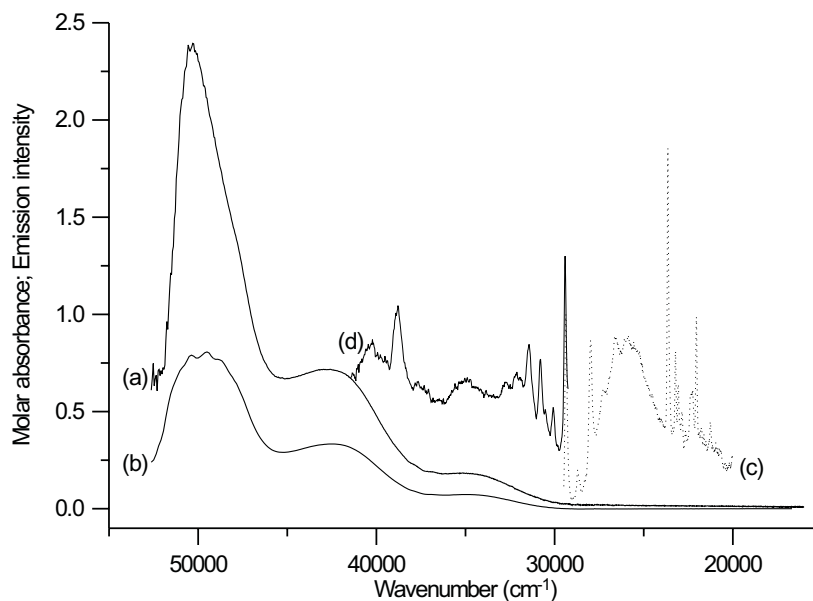


Figure 2. Absorption and emission spectra of DHP. (a, b) Absorption spectra of DHP in 3-methylpentane, $T=298$ K and 107 K, respectively; (c) Luminescence spectrum of DHP in n-heptane, $T=77$ K, excitation wavelength 270 nm; (d) Fluorescence excitation spectrum of DHP in n-heptane, $T=77$ K, emission wavelength 358 nm. The absorbance scale has been expressed in units of $10^5 \text{ dm}^3 \text{ mol}^{-1} \text{ cm}^{-1}$, the low-temperature spectrum has not been corrected for scattering. The intensities of luminescence and excitation spectra have been expressed in a.u., normalized at 29410 cm^{-1} ; the excitation spectrum has been vertically displaced to facilitate comparison.

assign the strong line at 23640 cm^{-1} to the $0-0 \text{ T}_1 \longrightarrow \text{S}_0$ transition, and other features of the spectrum in this spectral range to vibrational modes of the latter transition. Fluorescence excitation and phosphorescence excitation spectra were monitored at 27930 cm^{-1} ($0-1450 \text{ cm}^{-1}$) and at 23640 cm^{-1} ($0-0$ of the $\text{T}_1 \longrightarrow \text{S}_0$ transition). The resulting luminescence excitation spectra exhibit a long-wavelength peak at 29410 cm^{-1} (shifting to 29240 cm^{-1} in n-hexane). Within the experimental uncertainty, the peak is in resonance with the shortest-wavelength fluorescence peak at 29380 cm^{-1} and can therefore be attributed to the $0-0$ of the $\text{S}_1 \longleftarrow \text{S}_0$ transition. Beyond the $0-0$ peak, the excitation spectra consist of four relatively sharp bands between 30000 cm^{-1} and 31500 cm^{-1} and a few weaker and broader bands between 32000 cm^{-1} and 38000 cm^{-1} , followed by strong bands at 38820 cm^{-1} and 40500 cm^{-1} (*cf.* Table 1). The fluorescence lifetimes of DHP in n-heptane at room temperature are equal to $(1.34 \pm 0.02) \text{ ns}$, increasing to $(7.9 \pm 0.1) \text{ ns}$ at 77 K. The time constant of the decay of the emission at 23460 cm^{-1} ($0-0$ transition), measured at 77 K and attributed to the phosphorescence lifetime, was found equal to $(4.8 \pm 0.1) \text{ s}$.

The best resolution of the emission and excitation spectra of BDH was obtained in n-heptane matrix (see Fig. 3). To within the sensitivity of our apparatus, no detectable phosphorescence of BDH solutions was observed. The resolution and shape of the

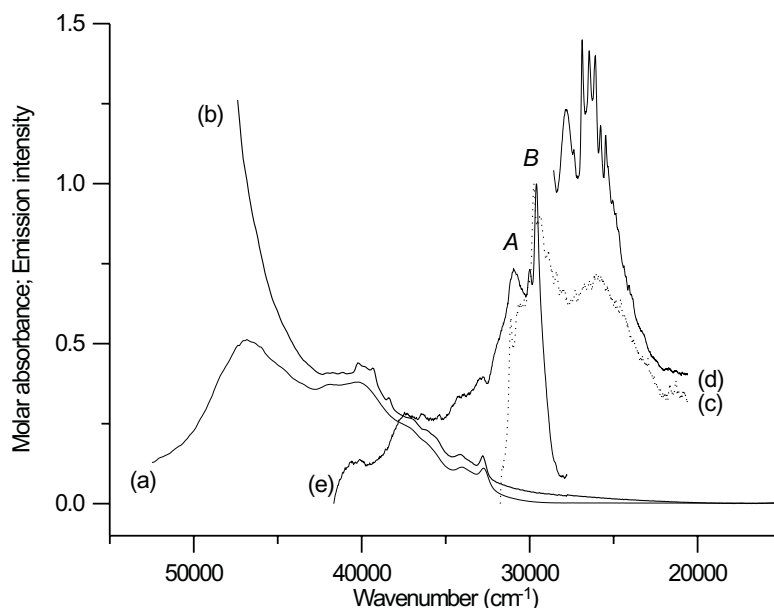


Figure 3. Absorption and emission spectra of BDH. (a, b) Absorption spectra of BDH in 3-methylpentane, $T=298$ K and 107 K, respectively; (c) Luminescence spectrum of BDH in n-heptane, $T=77$ K, excitation wavelength 280 nm; (d) Luminescence spectrum of BDH in n-heptane, $T=77$ K, excitation wavelength 338 nm; (e) Fluorescence excitation spectrum of DHP in n-heptane, $T=77$ K, emission wavelength 380 nm. The absorbance scale has been expressed in units of $10^5 \text{ dm}^3 \text{ mol}^{-1} \text{ cm}^{-1}$, the low-temperature spectrum has not been corrected for scattering. The intensities of luminescence and excitation spectra have been expressed in a.u., normalized at 30940 cm^{-1} ; curve (d) has been vertically displaced. The symbols 'A' and 'B' label the peaks attributed to 0-0 transitions of two emitting species.

fluorescence spectra were found wavelength-dependent. The excitation with a broad-band source at $(35700 \pm 500) \text{ cm}^{-1}$ yields a spectrum beginning with a sharp line at $\nu_{\text{em}} = 31100 \text{ cm}^{-1}$, and containing a strong line at 29600 cm^{-1} and a very broad band peaking at *ca.* 26000 cm^{-1} . Excitation at 29600 cm^{-1} gives the best resolved spectrum with a few strong and narrow peaks, shown in Fig. 3. The fluorescence excitation spectrum, monitored at $(26870 \pm 40) \text{ cm}^{-1}$, begins with a strong line at 29570 cm^{-1} , followed by weaker one at *ca.* 30000 cm^{-1} and a broader band at 30960 cm^{-1} . Within experimental resolution, the former line is in resonance with the strongest line in the fluorescence spectrum (29600 cm^{-1}), whereas the band is in resonance with the 31100 cm^{-1} line. The spectrum also contains a few ill-resolved bands, listed in Table 1. We also determined the fluorescence lifetimes of BDH. Fitting the curves measured at room temperature to monoexponential decays yielded $(2.35 \pm 0.04) \text{ ns}$ for the lifetime, whereas at 77 K the fluorescence decays were clearly non-monoexponential and could be reasonably fitted with two exponentials, the lifetimes amounting to 3.1 ns and 4.9 ns.

NMR: The ^1H chemical shifts presented in Table 2 are based on the analysis of ^1H , ^1H -COSY and ^1H , ^{13}C -COSY spectra (Fig. 4). ^1H signals from aromatic protons of DHP overlap at all temperatures, as can be seen on the spectra shown in Fig. 5, covering an appropriate region of ^1H NMR spectra of DHP at various temperatures. The ^{13}C spectrum allowed us to identify signals due to each carbon atom. No doubling nor coalescence of the signals was detected over the whole range of temperatures, we observed, however, a slight broadening of all signals. An example is presented in Fig. 6 showing a temperature evolution of the halfwidth of the peak at 152 ppm: between 183 K and 383 K the width changes by less than 7%.

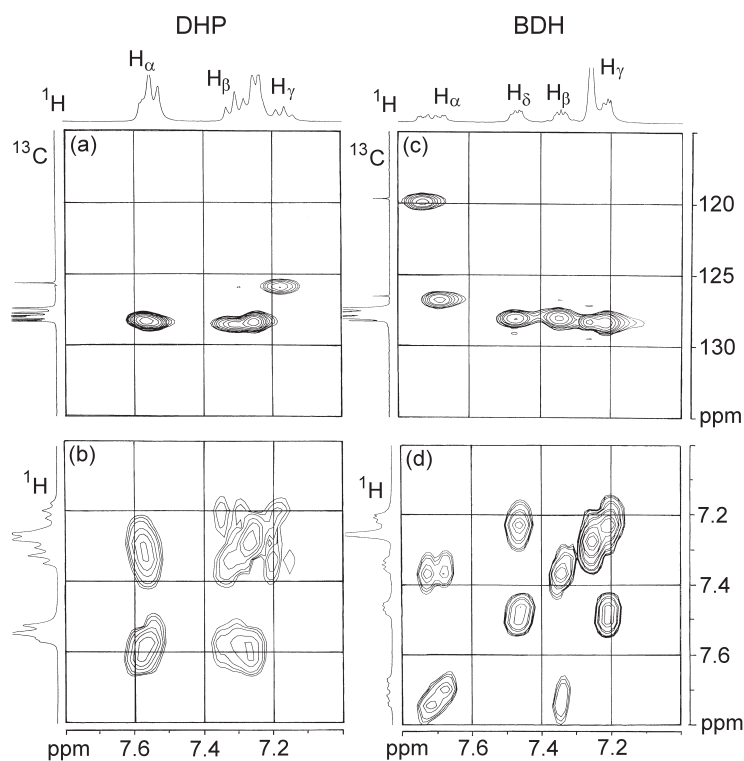


Figure 4. 2D NMR spectra of DHP and BDH in benzene- d_6 , at room temperature: (a) ^1H , ^{13}C COSY spectrum of DHP; (b) ^1H , ^1H COSY spectrum of DHP; (c) ^1H , ^{13}C COSY spectrum of BDH; (d) ^1H , ^1H COSY spectrum of BDH.

^1H spectra of BDH measured at room temperature in perdeuterated benzene (toluene) are characterized by two singlets, one from N- CH_3 at 2.70 ppm (2.76 ppm) and another from olefinic protons at 4.85 ppm (4.99 ppm), and a set of signals belonging to aromatic protons in the range 7.8–7.0 ppm. The signals from protons of the fluorene rings are well separated from those of the phenyl group. The aromatic rings of the fluorene moiety are nonequivalent; the feature is nicely expressed by different

chemical shifts of fluorene carbon signals, especially those for C₁ and C_{1'} signals (¹³C-NMR 119.7 and 110.3 ppm) and corresponding proton signals (¹H-NMR 7.50–7.60 ppm) – see Fig. 4. They do not coalesce even at 373 K (Fig. 7). The other proton and carbon signals overlap with solvent and with each other, being more difficult to interpret.

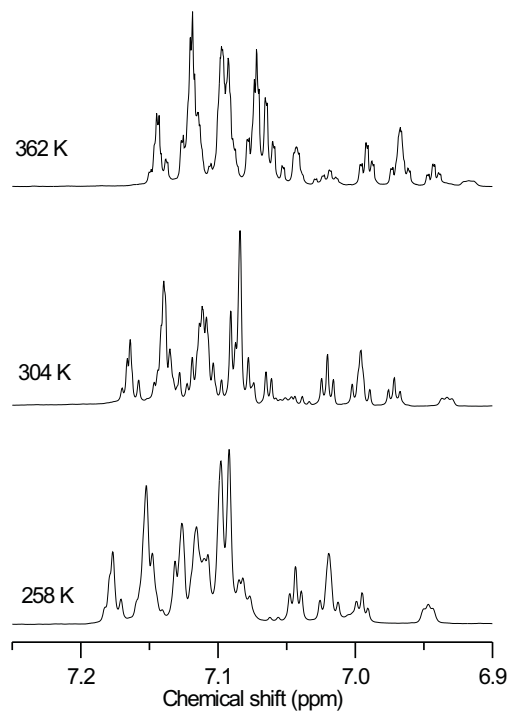


Figure 5. ¹H NMR spectra of DHP at various temperatures.

Table 2. Chemical shifts of protons in DHP and BDH at room temperature. Labeling of protons corresponds to that shown in Fig 1. All values are given in ppm.

	DHP		BDH	
	CDCl ₃	Benzene-d ₆	Benzene-d ₆	Toluene-d ₆
H ⁽¹⁾	7.58	7.55	7.72 7.68	7.61 7.56
H ⁽²⁾	7.40	7.31	7.64	7.24
H ⁽³⁾	7.21	7.16	7.25	7.01
H ⁽⁴⁾			7.46	7.36
Phenyl protons	7.35	7.25	7.25	7.13
Olefinic protons	5.30	5.56	4.99	4.85
N-CH ₃	2.62	2.26	2.76	2.70

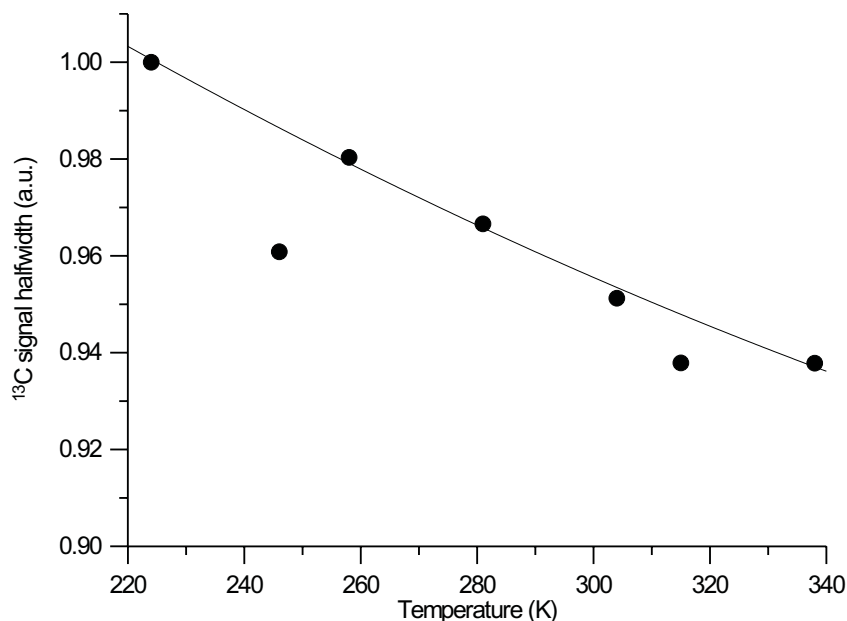


Figure 6. Temperature dependence of the 152 ppm ^{13}C signal halfwidth in DHP. The values have been normalized at 224 K. The line serves only to guide the eye.

In spite of all similarities between DHP and BDH observed in earlier photochemical experiments, several features of electron and NMR spectra presented in this paper point to discernible differences between the molecules under study. Within the entire temperature range covered by our experiments, DHP shows only a single set of carbon and proton resonances for two phenyl groups attached to the central ring in the position 4. Thus, although the formal symmetry of the molecule is C_s , it assumes an average C_{2v} symmetry on the NMR time scale, due to a conformational freedom. ^1H , ^1H -COSY and ^1H , ^{13}C -COSY spectra of DHP support this conclusion. There is also no significant change of the linewidth of the ^{13}C signal at 152.00 ppm: over the entire temperature range the linewidth did not change by more than 7% (*cf.* Fig. 6). Thus, one may conclude that NMR spectra of DHP point to a substantial freedom of orientation of side phenyl groups and, in general, to a conformational freedom of the molecule at room temperature. An inspection of the temperature dependence of the spectra indicates that this feature is preserved down to at least 183 K.

The behaviour of BDH is different: all features of the NMR spectra unambiguously point to a nonequivalence of the two side rings of the fluorene moiety. On the NMR time scale, the molecule possesses the symmetry not higher than C_s . At elevated temperatures (up to 373 K) the spectra do not change significantly, except for a slight broadening, indicating that the energy barrier for the inversion of the central dihydropyridine ring should be quite high. Interestingly, the difference between the chemical shifts of l and l' protons of the fluorene moiety decreases upon cooling the sample

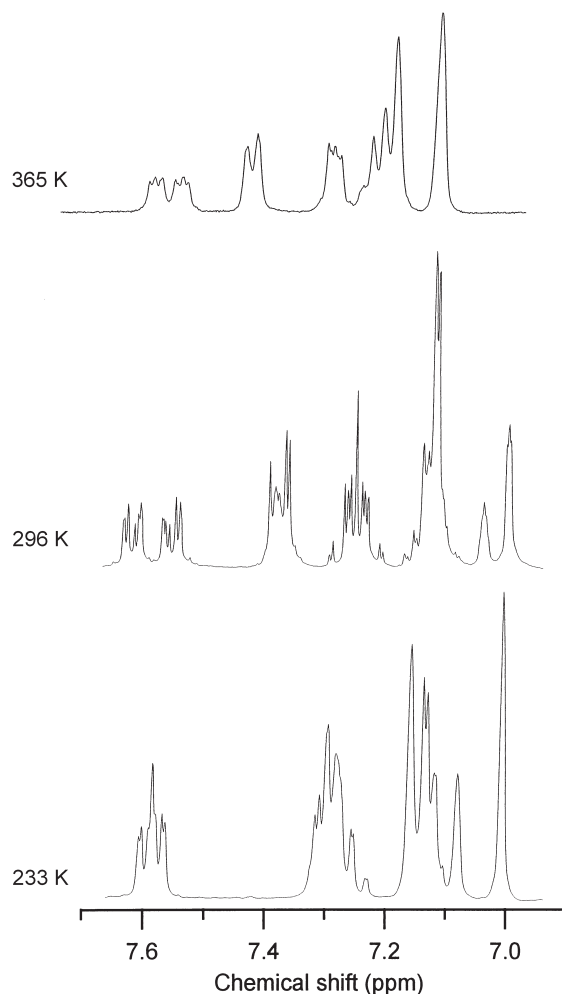


Figure 7. ^1H NMR spectra of BDH at various temperatures.

(*cf.* Fig. 7). At 213 K the signals merge into a triplet. At present, we cannot offer any convincing explanation for this finding.

The resonance agreement of the first lines in the luminescence excitation spectra and in the fluorescence spectrum of DHP molecule allows one to attribute them to 0-0 of the $S_1 \longleftrightarrow S_0$ transition, the energy of the first excited singlet state amounting to *ca.* 29400 cm^{-1} . A comparison of the low-temperature luminescence excitation spectra of DHP in an *n*-heptane matrix with the absorption spectra in 3-methylpentane solution or glass (*cf.* Fig. 2) indicates that the entire structure, visible in the excitation spectra, associated with transitions to higher vibronic levels of the S_1 state and to higher excited singlet states, is completely hidden in the absorption spectra under a broad

band peaking at *ca.* 34800 cm⁻¹. The effect can be rationalized taking into account different morphologies of matrices: *n*-heptane is polycrystalline at 77 K, whereas 3-methylpentane forms a glassy matrix at 118 K. The position of the next intense absorption band with the onset at *ca.* 40000 cm⁻¹ is in a reasonable agreement with an intense band observed in the excitation spectrum at 38820 cm⁻¹.

Apart from the transitions within the singlet manifold, position of the line corresponding to the 0-0 of the T₁ → S₀ transition has also been marked. The singlet-triplet splitting in DHP was determined to amount to 5780 cm⁻¹, a value typical of large organic molecules.

The analysis of the excitation spectra of DHP allows one to assign tentatively the peaks appearing between the 0-0 and 31500 cm⁻¹ (and possibly also two weaker peaks at 32160 cm⁻¹ and 32790 cm⁻¹) to vibronic transitions within the S₁ ←→ S₀ manifold. The peaks beyond 33000 cm⁻¹ are probably associated with transitions to higher excited states. Unfortunately, an unambiguous assignment is difficult in this case in view of discrepancies between the experimental data and results of quantum-chemical calculations (see Table 1). The quantum-chemical calculations reasonably well reproduce the intensity pattern, the agreement of the energy scale is, however, far worse, in particular for the lowest transition: the calculated energy of the S₁ state exceeds the experimentally determined value attributed to the 0-0 of the S₁ → S₀ transition by *ca.* 4000 cm⁻¹. The agreement is much better for higher singlet states and the T₁ state, where the difference does not exceed 750 cm⁻¹. The reason for such a discrepancy could be sought in the fact that the quantum chemical methods, calculating vertical transitions are always likely to overestimate the transition energies. Moreover, the effect of the environment, neglected in the present calculations, can substantially contribute to this difference. In particular, environment-induced deformations of the central moiety are likely to result in important shifts of the energy levels as may be inferred from the results obtained for DHP.

A resonance agreement between emission and excitation spectra has also been found in BDH; in contrast to DHP, however, the agreement has been observed for two bands (labelled A and B in Fig. 3). This feature points to a purely electronic character of the transitions associated with both bands, their presence cannot be attributed, however, to the existence of different Shpol'skii sites (*i.e.*, sites containing geometrically identical guest molecules built into slightly different host environment). The energy difference between the bands, 1350 cm⁻¹, greatly exceeds values typical of the Shpol'skii splitting, which do not exceed a few hundred cm⁻¹. This feature can be rationalized assuming a co-existence of two emitting species; we postulate that these species are two forms of BDH.

There exist several results supporting the above hypothesis, major support coming from results of quantum-chemical calculations. As was already mentioned, in both molecules under study the central (dihydropyridine) rings are non-planar [2,8,15]. This result was also confirmed by MNDO calculations performed in this work. Our calculations showed that there exists only one stable structure of DHP, whereas for a more rigid molecule of BDH the calculations predict the existence of

two similar but distinct structures shown in Fig. 8. The structure labelled 'B' is more stable but the difference of ground-state energies between 'A' and 'B' amounts to 2.42 kJ/mol only. Consequently, one may expect a coexistence of two forms. Energies of electronic states, calculated for both forms, are shown in Table 1. The calculations yield again overestimated energies of the lowermost levels, they nevertheless correctly predict the energy difference between the $S_1 \longrightarrow S_0$ transitions in the conformers. Thus, we attribute the two origins detected in the spectra of BDH to the existence of two conformers of slightly different yet well defined geometries built into the polycrystalline solvent matrix.

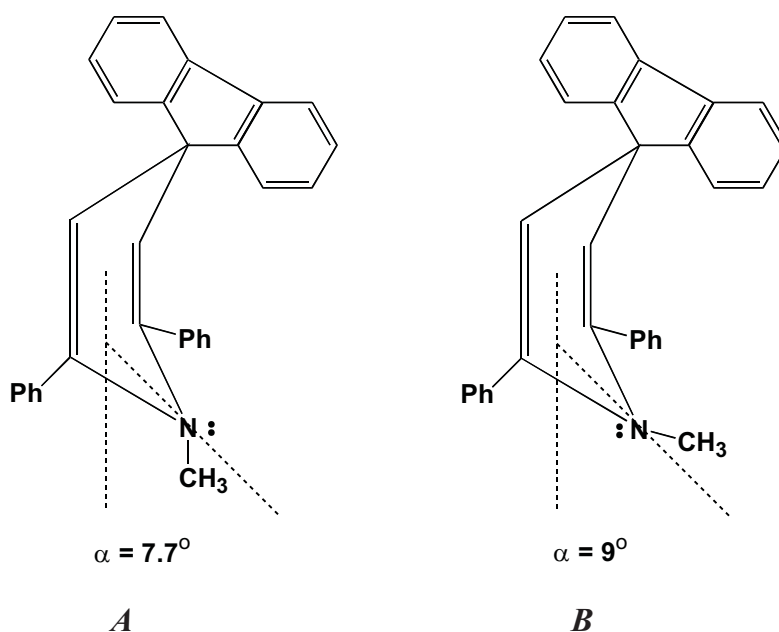


Figure 8. Schematic presentation of two molecular structures of BDH. See text for discussion.

Other experimental details also speak in favour of our hypothesis. The 'A' band in the fluorescence excitation spectrum is broader than the 'B' band, probably due to overlapping of the purely electronic transition in A-type molecules with an electronic-vibronic transition in B-type molecules. Finally, the bi-exponential decay of the fluorescence measured at 77 K in polycrystalline solutions of BDH in n-heptane may be taken for an additional result supporting the hypothesis of two emitting species being present in the system – at least at low temperatures.

Our results confirm that BDH molecules enjoy much less freedom than those of DHP. The difference, clearly visible in NMR experiments, is due to the chemical bond linking the position-4 phenyls in the former molecule. Moreover, the enhanced rigidity of BDH seems to be responsible for the appearance of two species in its low-temperature emission spectra. We assume that these species are BDH molecules

with slightly different central dihydropyridine moieties. Interestingly, we could not identify any signature of coexistence of two species in the NMR spectra. The explanation should probably be sought in different sensitivities of the two methods to small distortions of the central ring.

Acknowledgments

This work was supported in part by the Polish State Committee for Scientific Research (grant No 3 T09A 106 19), by the Wrocław University of Technology and by the Grant Agency of the Academy of Sciences of the Czech Republic. The luminescence measurements were carried out on the equipment purchased by the Foundation for Polish Science. ES thanks DAAD for a scholarship, and Professor G. Hohlneicher and Dr. H. Schmickler (University of Cologne) for hospitality and permission to carry out some absorption and NMR measurements. The authors thank Professor J. Kuthan and Dr. S. Böhm (Prague Institute of Chemical Technology) for the gift of the materials used in this study.

REFERENCES

1. Ohashi Y. (Ed.), *Reactivity in Molecular Crystals*, Kodansha and VCH, Tokyo and Weinheim, 1994, Chap. 5.
2. Nešpůrek S., Sworakowski J., Lipiński J., Böhm S. and Kuthan J., in: Kajzar F. and Agranovich V.M. (Eds.), *Multiphoton and Light Driven Multielectron Processes in Organics: New Phenomena, Materials and Applications*, Kluwer, Dordrecht 2000, p. 261.
3. Sworakowski J., Nešpůrek S., Lipiński J., Śliwińska E., Lewanowicz A. and Olszowski A., in: Kajzar F. and Agranovich V.M. (Eds.), *Multiphoton and Light Driven Multielectron Processes in Organics: New Phenomena, Materials and Applications*, Kluwer, Dordrecht 2000, p. 249.
4. Maeda K., Nakamura M. and Sakai M., *J. Chem. Soc. Perkin Trans. I*, 837 (1983).
5. Iwasaki F., Watanabe T. and Maeda K., *Bull. Chem. Soc. Japan*, **60**, 1255 (1987).
6. Shibuya J., Nabeshima M., Nagano H. and Maeda K., *J. Chem. Soc. Perkin Trans. II*, 1607 (1988).
7. Nešpůrek S., Schwarz M., Böhm S. and Kuthan J., *J. Photochem. Photobiol. A*, **60**, 345 (1991).
8. Böhm S., Hocek M., Nešpůrek S. and Kuthan J., *Coll. Czech. Chem. Commun.*, **59**, 263 (1994).
9. Nešpůrek S. and Schnabel W., *J. Photochem. Photobiol. A*, **81**, 37 (1994).
10. Nešpůrek S., Böhm S. and Kuthan J., *Mol. Cryst. Liq. Cryst.*, **246**, 139 (1994).
11. Lewanowicz A., Lipiński J., Nešpůrek S., Olszowski A., Śliwińska E. and Sworakowski J., *J. Photochem. Photobiol. A*, **121**, 125 (1999).
12. Sworakowski J., Nešpůrek S., Lipiński J. and Lewanowicz A., *J. Photochem. Photobiol. A*, **129**, 81 (1999).
13. Śliwińska E. and Sworakowski J., *Adv. Mat. Opt. Electron.*, **9**, 167 (1999).
14. Sworakowski J., Nešpůrek S., Lipiński J., Lewanowicz A. and Śliwińska E., *Mol. Cryst. Liq. Cryst.*, **356**, 163 (2001).
15. Hašek J. and Ondráček J., *Acta Cryst. C*, **46**, 1256 (1990).
16. Dähne S., Becker W., Scholtz W., Teuchner W., Lucht H. and Schneider H., *Feingerätetechnik*, **29**, 463 (1980).
17. Šebek P., Nešpůrek S., Hrabal R., Adamec M. and Kuthan J., *J. Chem. Soc. Perkin Trans. II*, 1310 (1992).
18. Dewar M.J.S. and Thiel W., *J. Am. Chem. Soc.*, **99**, 4899 (1977).
19. Lipiński J., *Int. J. Quantum Chem.*, **34**, 423 (1988).